Resolution improvement of two-layer optical coherence tomography via neural network

1st Kun Wang
Wuhan National Laboratory for Optoelectronics & School of Optical and Electronic Information, Huazhong University of Science and Technology Optics Valley Laboratory
Wuhan, China
m202173365@hust.edu.cn

2nd Liang Xu
Wuhan National Laboratory for Optoelectronics & School of Optical and Electronic Information, Huazhong University of Science and Technology Optics Valley Laboratory
Wuhan, China
xuliang180534@163.com

3rd Chen Liu
Wuhan National Laboratory for Optoelectronics & School of Optical and Electronic Information, Huazhong University of Science and Technology Optics Valley Laboratory
Wuhan, China
chenliu_wnlo@hust.edu.cn

4th SaiYang Liu
Wuhan National Laboratory for Optoelectronics & School of Optical and Electronic Information, Huazhong University of Science and Technology Optics Valley Laboratory
Wuhan, China
m202273385@hust.edu.cn

5th Chi Zhang*
Wuhan National Laboratory for Optoelectronics & School of Optical and Electronic Information, Huazhong University of Science and Technology Optics Valley Laboratory
Wuhan, China
chizheung@hust.edu.cn

6th Xinliang Zhang
Wuhan National Laboratory for Optoelectronics & School of Optical and Electronic Information, Huazhong University of Science and Technology Optics Valley Laboratory
Wuhan, China
xlzhang@mail.hust.edu.cn

***Abstract*—We propose a deep learning method to enhance the axial resolution between two-layer of optical coherence tomography images. Experiments are conducted on two-layer samples and demonstrated that it can improve the resolution by quadruple.**

***Keywords*—optical coherence tomography, deep learning, axial resolution**

I. Introduction

Optical coherence tomography (OCT) is a non-invasive imaging technique that provides 3D information on the optical scattering properties of living biological tissue [1]. OCT has been widely used in clinical applications and has gained considerable attention since its inception. Resolution is one of the key parameters of OCT systems, which includes both horizontal and axial resolution. The axial resolution of an OCT system is related to the light source, which requires a smaller center wavelength or a larger spectral bandwidth. A Ti:Al_2O_3 sapphire laser built by A. Unterhuber et al. was applied with a center wavelength of 850 nm and a spectral bandwidth of 176 nm, achieving an axial resolution of 3 µm in space[2]. P. R. Herz et al. combined a compact bandwidth-limited Cr^{4+}: Forsterite laser with a nonlinear fiber to generate a spectral bandwidth greater than 200 nm at a center wavelength of 1250 nm, achieving an axial resolution of 3.7 µm[3]. Currently, high frame rate and large depth OCT is implemented using swept-source OCT (SS-OCT). However, increasing the axial resolution by changing the frequency range and center wavelength of the swept-source is complex, and alternative approaches are adopted to improve the axial resolution of SS-OCT systems.

Recently, the rapid development of artificial intelligence has led to numerous efforts to apply deep learning to OCT, resulting in significant progress. G. Ni et al. reduced speckle noise by generative adversarial network [4]. S. Soltanian-Zadeh et al. used weakly supervised learning to enhance the correlation between the structure and function of GCL cells [5]. R. Liu et al. applied convolutional neural network and fully connected neural network to optical imaging for measuring blood oxygen saturation, improving image quality and measurement accuracy compared to the original OCT imaging method [6]. A. V. Varadarajan, et al. trained a deep learning model to detect ci-DMe cells using only 2D images, simplifying the detection process without the need for 3D images, to detect simply [7]. A. Ozcan et al. improved imaging speed without sacrificing resolution and signal-to-noise ratio by downsampling spectral domain data and using a modified U-Net architecture with residual connections to recover and image the downsampled data [8]. The integration of deep learning algorithm and OCT has had a positive impact on the development.

This paper proposes a method to train a neural network model with a large amount of prior knowledge, the trained model can import small bandwidth signal data and predict data of the large spectral bandwidth, expanding the detection bandwidth and improving the axial resolution of the system. Two-layer cover slip sample data was used to verify the proposed method, which achieved four times improvement in the axial resolution of the SS-OCT system without modifying any hardware.

II. Principle and Results

To demonstrate a deep learning algorithm to improve the axial resolution of an SS-OCT system, a two-layer cover slip was employed as the sample under test. First, the time-domain interferometric data for a two-layer cover slip was generated via simulation using Matlab and the actual system parameters of the SS-OCT setup, according to the following equation:

$$I(t)=2\exp\left[-4\ln 2\left(\frac{t}{T_0}\right)^2\right]\left\{\cos\left[\frac{\Delta\omega\delta t_1}{T_0}\left(t-\frac{\delta t_1}{2}+\frac{\omega_0 T_0}{\Delta\omega}\right)\right]+\cos\left[\frac{\Delta\omega\delta t_2}{T_0}\left(t-\frac{\delta t_2}{2}+\frac{\omega_0 T_0}{\Delta\omega}\right)\right]\right\} \tag{1}$$

National Key Research and Development Program of China (Grant Nos. 2022YFF0705904) and the National Natural Science Foundation of China (Grant Nos. 62075072, and 61927817).

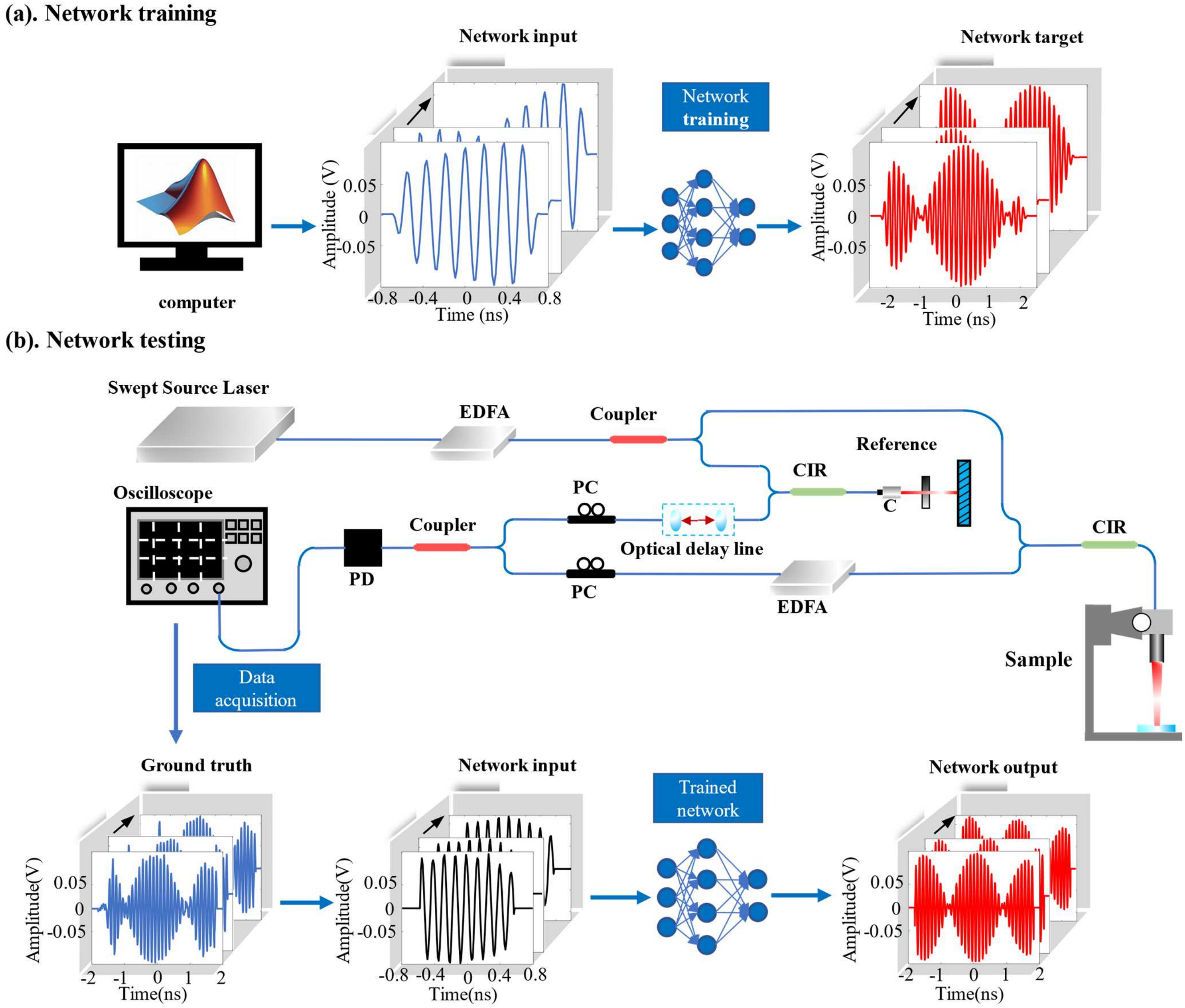

Fig. 1. The schematic diagram of the experiment. (a) Network training, simulated data as training data for neural networks. (b) Network testing, acquiring two-layer coverslip data using an SS-OCT system for neural network model testing.

where $\delta t_1=2d_1/c$, $\delta t_2=2d_2/c$, d_1 and d_2 represents the absolute depth of each layer, c represents the speed of light in air, $T_0=1/f_{rep}$. The system parameters of SS-OCT are as follows: the swept-source has a central wavelength of 1550 nm, a sweep range of 40nm, a repetition rate of 100 MHz. The axial resolution of the system has been characterized as 36 μm in air, and the sampling rate of signal acquisition is 80 GSa/s. The training of the model is shown in Fig. 1(a), where the sweep range is set to generate corresponding narrow-band and broadband signals. In the experiment, a narrow-band sweep range of 10 nm is chosen as the input of the neural network, while sweep ranges of 20 nm, 30 nm, and 40 nm are used as the output of the neural network for the corresponding broadband signals that are double, triple, and four-fold of the original bandwidth, respectively. By exploring various situations at different absolute depths, a large amount of corresponding input and output data for the neural network are generated, and it is served as the training data for the deep learning model. We had trained separate neural network models for bandwidths that were expanded by double, triple, and four-fold.

The experimental testing process is shown in Fig. 1(b), we acquired interference fringes from a two-layer cover slip sample using the SS-OCT system. During the actual sample data acquisition process, to adjust the reference arm to ensure that the absolute depth of the sample was within the depth range that our model was trained. The collected real data is acted as the ground truth, and the small bandwidth signal filtered from the real data is acted as the input data of the model, then the neural network predicted the corresponding to the signal with the expanded bandwidth. To quantify the performance of the model in expanding the detection bandwidth, generating 2D images of the 102 frames temporal data predicted by neural network model and real data obtained by the existing configuration. From the image perspective, we evaluated the accuracy of neural network output data by calculating two quantitative indicators: peak signal-to-noise ratio (PSNR) is defined as:

$$PSNR = 10\times\log_{10}\left(\frac{MAX_I^2}{MSE}\right) \tag{2}$$

where MAX_I is the maximum possible pixel value of the ground truth image, and mean squared error (MSE) between the two images being compared is defined as:

$$MSE = \frac{1}{n^2}\sum_{i=0}^{n-1}\sum_{j=0}^{n-1}\left[I(i,j)-K(i,j)\right]^2 \quad (3)$$

where I is the target image, and K is the image that is compared with the target. The structural similarity index measure (SSIM) is defined as:

$$SSIM = \frac{(2\mu_a\mu_b + C_1)(2\sigma_{a,b} + C_2)}{(\mu_a^2 + \mu_b^2 + C_1)(\sigma_a^2 + \sigma_b^2 + C_2)} \quad (4)$$

where μ_a and μ_b are the mean values of a and b, which represent the two images being compared, σ_a and σ_b are the standard deviations of a and b, $\sigma_{a,b}$ is the cross covariance, respectively, and C_1 and C_2 are constants that are used to avoid division by zero.

In addition, we also compared the simulated test data with the experiment data by randomly selected single frame time-domain interference data. The comparison was conducted to evaluate the accuracy between the simulation results and the actual data.

As shown in Fig. 2, this paper presents the test results of simulated and real narrowband data, which were expanded by a neural network model to two-fold, triple, and four-fold of their original bandwidth. Quantitative analysis reveals that the real data collected from experiments, due to the possible presence of high-order dispersion that was not completely eliminated, yields slightly inferior results compared to the simulated data. However, in the image domain, the PSNR of the 2D neural network output images fall within the range of 20~30 dB, which is generally acceptable, and the SSIM metric, which focuses on the structural similarity between two images and has a value between 0 and 1 (where 1 represents identical images), shows that the SSIM of the test output data images is above 0.9, indicating satisfactory performance. Additionally, in the frequency domain, the peak frequencies of the neural network output data and the corresponding ground truth are well aligned. These quantitative and qualitative results verify that the neural network prediction of large bandwidth data is effective, thereby demonstrating the feasibility of using deep learning to expand detection bandwidth and improve axial resolution. Based on the experimental results, the axial resolution of SS-OCT systems for the single-layered cover glass sample can be improved from 151 to 38 μm, with a four times improvement in axial resolution.

III. Conclusions

We propose a novel approach for improving the axial resolution of OCT images with two-layer structure. Experimental verification is conducted on a two-layer cover slip sample. By utilizing deep learning without modifying the hardware configuration, to improve the axial resolution of the SS-OCT system. In future work, it is expected that this method can be applied to improve the axial resolution of a 40-nm spectral bandwidth OCT system equals to that of the 160-nm spectral bandwidth, thereby improving the axial resolution of the from 40 to 10 μm. However, this method may face significant limitations when applied to complex biological tissue samples and may not achieve the desired effect of improving axial resolution. Therefore, further exploration of this issue is needed in future work, with a focus on leveraging deep learning to improve the axial resolution of OCT systems.

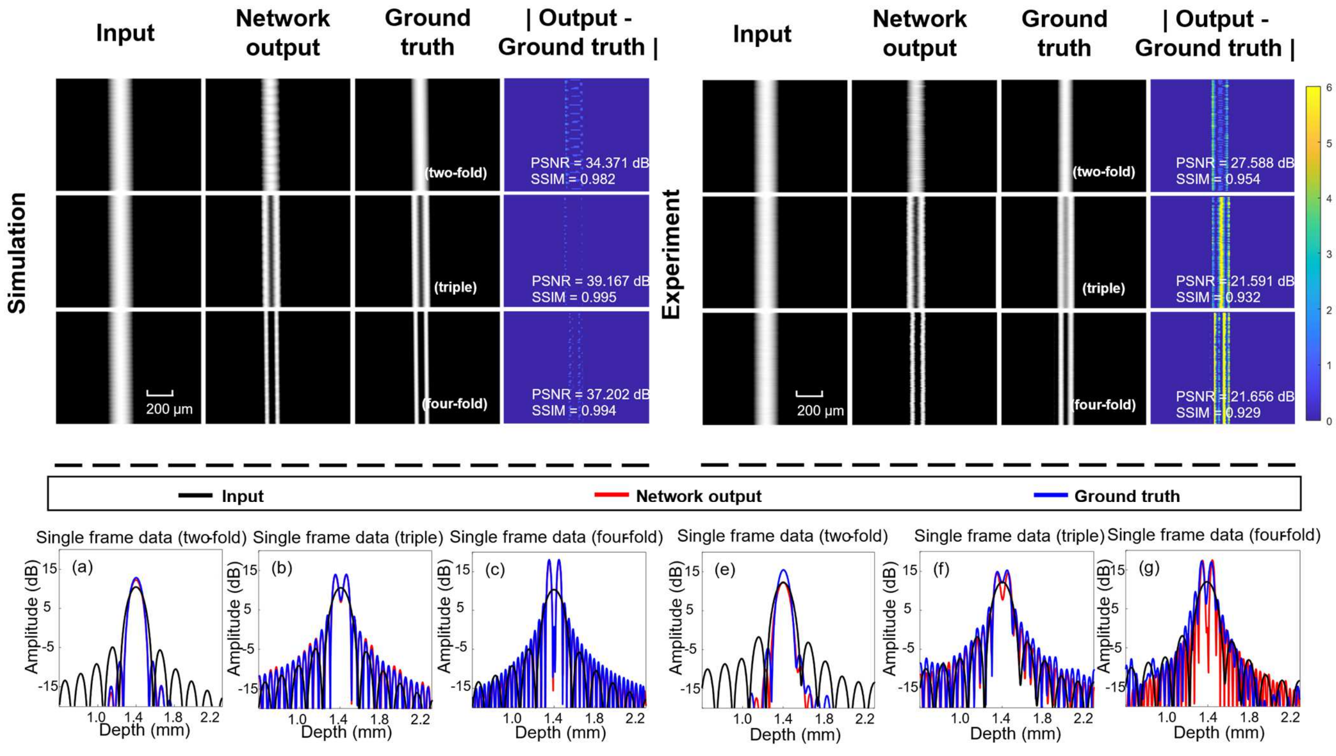

Fig. 2. Experimental test results, where simulation indicates the test results using simulated data and experiment indicates the test results using real data, the bar in grayscale represents the difference values between the two images. In particular, (a), (b), and (c) represent the test results of single-frame simulated data, while (e), (f), and (g) represent the test results of single-frame real data.

ACKNOWLEDGMENT

This work was supported by grants from the National Key Research and Development Program of China (Grant Nos. 2022YFF0705904) and the National Natural Science Foundation of China (Grant Nos. 62075072, and 61927817).

REFERENCES

[1] D. Huang, E. A. Swanson, C, P. Lin, J. S. Schuman W. G. Stinson, W. Chang, M. R. Hee, T. Flotte, K. Gregory, and C. A. Puliafito, "Optical coherence tomography," Science 254, 1178-1181, 1991.

[2] A. Unterhuber, B. Považay, B. Hermann, H. Sattmann, W. Drexler, V. Yakovlev, G. Tempea, C. Schubert, E. M. Anger, P. K. Ahnelt, M. Stur, J. E. Morgan, A. Cowey, G. Jung, T. Le, and A. Stingl, "Compact, low-cost Ti:Al_2O_3 laser for in vivo ultrahigh-resolution optical coherence tomography," Opt. Lett. 28, 905-907, 2003.

[3] P. R. Herz, Y. Chen, A. D. Aguirre, J. G. Fujimoto, H. Mashimo, J. Schmitt, A. Koski, J. Goodnow, and C. Petersen, "Ultrahigh resolution optical biopsy with endoscopic optical coherence tomography," Opt. Express 12, 3532-3542, 2004.

[4] G. Ni, Y. Chen, R. Wu, X. Wang, M. Zeng, and Y. Liu, "Sm-Net OCT: a deep-learning-based speckle-modulating optical coherence tomography," Opt. Express 29, 25511-25523, 2021.

[5] S. Soltanian-Zadeh, K. Kurokawa, Z. L. Liu, F. Zhang, O. Saeedi, D. X. Hammer, D. T. Miller, and S. Farsiu, "Weakly supervised individual ganglion cell segmentation from adaptive optics OCT images for glaucomatous damage assessment," Optica 8, 642-651, 2021.

[6] R, Liu, S. Cheng, L. Tian, J. Yi. "Deep spectral learning for label-free optical imaging oximetry with uncertainty quantification," Light Sci Appl, 8, 102, 2019

[7] A. V. Varadarajan, P. Bavishi, P. Ruamviboonsuk, P. Chotcomwongse, G. S. Corrado, L. Peng, D. R. Webster. "Predicting optical coherence tomography-derived diabetic macular edema grades from fundus photographs using deep learning," Nat Commun, 11, 130, 2020.

[8] Y. Zhang, T. Liu, M. Singh, E. Cetintas, Y. L. Luo, Y. Rivvenson, K. V. Larin, A.Ozcan. "Neural network-based image reconstruction in swept-source optical coherence tomography using undersampled spectral data," Light Sci Appl 10, 155, 2021.